Photoemission evidence of electronic stabilization of polar surfaces in K_3C_{60}

R. Hesper, L. H. Tjeng, A. Heeres, and G. A. Sawatzky
Solid State Physics Laboratory, Materials Science Centre, University of Groningen, Nijenborgh 4, 9747 AG Groningen, the Netherlands
(Received 19 April 2000)

We present a detailed investigation of the surface electronic structure of solid K_3C_{60} in connection with its electronic transport properties. We find that the conductivity is extremely sensitive to the K concentration of the surface layer, and that the best-conducting samples with the highest superconducting transition temperatures have surfaces with the highest density of states at the Fermi level as measured by photoemission. The C_{60} ions at the surface have, however, a valence that deviates appreciably from the $3-$ bulk value, namely $2.5-$ or even $1.5-$, depending on the preparation procedure. We attribute this as being the result of an electronic rather than an atomic surface reconstruction to avoid the divergence of the electrostatic potential associated with the polar (111) surface termination of K_3C_{60}. We argue that such a mixed-valence surface should always be a metal, irrespective of whether the bulk is a metal or a Mott-Hubbard insulator.

I. INTRODUCTION

There exists a large body of literature concerning the photoemission spectra of alkali-metal-doped C_{60} (Refs. 1–12). This forms, however, a rather mixed set of experimental data and does not necessarily provide clear information for the study of the electronic structure of these materials. Especially if we compare the spectral features close to the Fermi level (E_F) of samples that are supposed to consist of the metallic and superconducting phase K_3C_{60}, we notice that there is a large divergence, both in line shape and spectral weight, in published data, as depicted in Fig. 1. Nearly all of the studies made use of samples that were prepared *in situ*, so the reason for the divergence in the data must lie in a strong dependence on the preparation method and the conditions during preparation. Unfortunately, *in situ* characterization of the samples was not given in most of these works, using, for example, electrical conductivity measurements in order to establish at least that the material behaves like a metal and becomes a superconductor at around 19 K.

Also on the theoretical side there are several questions concerning the electronic structure of K_3C_{60}. Density functional calculations[13] predict that the sixfold degenerate t_{1u} band, derived from the lowest unoccupied molecular orbital (LUMO) of C_{60}, becomes half-filled due to the transfer of charge from the potassium, and that this occurs in a rigid-band-like manner producing a metallic LUMO-derived band with an occupied part that is less than 0.3 eV wide. Existing photoemission data shows, however, widths of the order of 1.2 eV for the occupied part of the LUMO, which could be taken as an indication for the presence of strong electron correlation effects.[14] The presence of these is also suggested by the fact that K_4C_{60} is an insulator with an appreciable band gap,[15] while density functional calculations predict it to be a metal.[16] Yet, it is far from clear how these correlation effects affect the electronic structure of K_3C_{60}. A simple estimate within the Mott-Hubbard framework, using the experimentally derived value for the on-site Coulomb energy U of 1.6 eV (Ref. 14), suggests that K_3C_{60} should be an insulator just like K_4C_{60}, since the LUMO bandwidth W is smaller than U. To reason that K_3C_{60} is metallic, one has to assume appreciable nonstoichiometry[14,17] or one has to use more elaborate calculations that take into account the effective orbital degeneracy together with perhaps a smaller value for U (Refs. 18–23). To predict the line shape of the valence band spectrum is even a more difficult task, because of the complexity of a three-dimensional system with both appreciable U and W, as well as orbital degeneracy and the influence of electron-phonon coupling.

In this paper we present the results of a detailed photo-

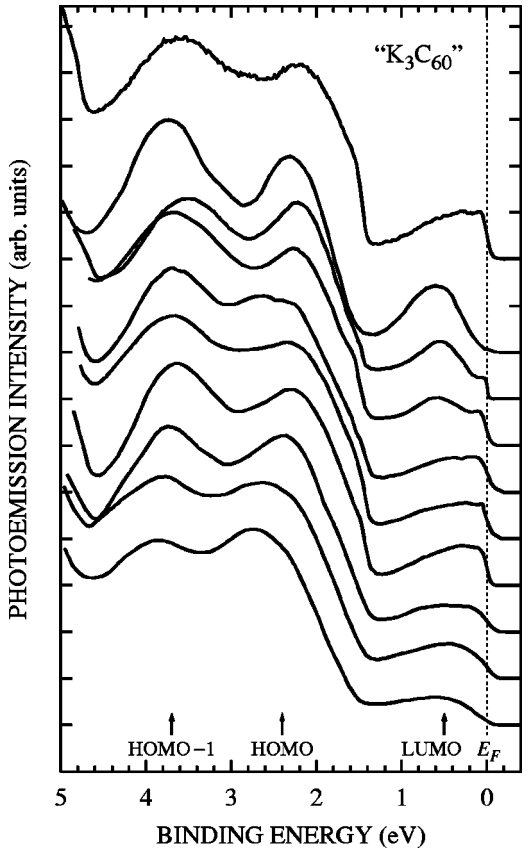

FIG. 1. Collection of various photoemission spectra of K_3C_{60} as found in the literature (Refs. 1–12), normalized to the HOMO peak height. The top spectrum is from the present work (Fig. 4).

emission study on K_3C_{60} solids for which we have adopted an approach from the field of transport measurements that has proven to provide samples with reproducible and verifiable quality. We have prepared our samples in such a way that the resistivity as a function of K concentration is at a minimum and verified that the temperature dependence is metallic and that the superconducting transition temperature is around 19 K with a transition width of less than 1 K. The preparation, the monitoring by conductivity measurements, and the photoemission experiments themselves were all carried out *in situ* under 10^{-11} mbar ultrahigh vacuum (UHV) conditions. We have observed that the conductivity is extremely sensitive to the K concentration at the surface. We have found that the valence of the C_{60} ions at the surface is different from those in the bulk, and that therefore the observed photoemission spectra are *not* representative for bulk K_3C_{60}. The completely different electronic structure of the surface layer is attributed to an intrinsic property of the system, namely a macroscopic charge redistribution neutralizing the divergent electrostatic potential associated with the polar (111) surface termination of K_3C_{60}. We argue that such mixed-valence surfaces have quite unique physical properties, and that their electronic structure should be described by a Hubbard model with 50% doping.

II. EXPERIMENT

The experiments were performed in a combined photoemission and conductivity setup, with *in situ* sample preparation facilities and a base pressure better than 5×10^{-11} mbar throughout. Samples were made by evaporating C_{60} from a thoroughly degassed Knudsen cell at a rate of approximately 1 monolayer per minute onto Al_2O_3 substrates, kept at a temperature of 200 °C to promote the formation of crystalline films.[24] The thickness of the films ranged from 50 to 200 nm. The evaporation rate was calibrated with a quartz crystal balance before and after the film deposition. The quartz balance calibration was in turn verified *ex situ* by measuring the thickness of a test C_{60} film using an electron microscope. Potassium was emitted from a thoroughly degassed SAES getter source with the substrate kept at 200°C.

The substrates used were rectangular, randomly oriented Al_2O_3 single crystal plates, polished to a surface roughness of less than 10 Å, with typical dimensions of $12\times5\times0.5$ mm. Electrical contact pads, typically consisting of 80 nm Ag on a 20 nm Ti binding layer, were evaporated *ex situ* on the substrates prior to introduction into the vacuum system. For the contacts pads a two-probe configuration was used, connected to separate current and voltage wires leading outside. No nonlinearities or deviations from earlier true four-probe measurements were observed. The substrates were clamped with stiff molybdenum springs onto a copper sample holder mounted on a Janis Supertran continuous flow cryostat. Temperature was measured with a Si diode mounted on the cryostat and a Pt-1000 resistor directly next to the sample. Because of the required free access for evaporation and spectroscopy purposes, no thermal shielding was employed. Nevertheless, since the measured T_c of the best doped films was always within 1 K from the highest literature values, we are confident that the actual sample temperature never deviated more that 1 K from the measured one.

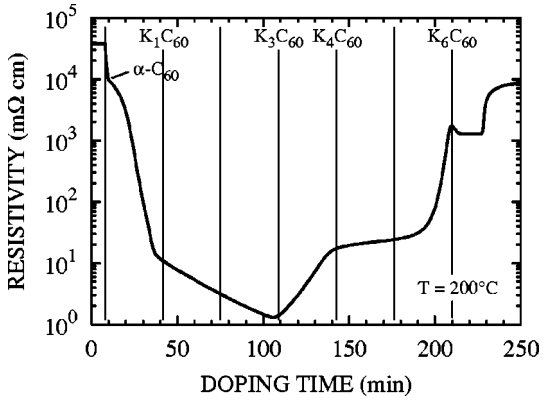

FIG. 2. Resistivity of a 50 nm thick C_{60} film during potassium doping to K_6C_{60} at a temperature of 200 °C.

Electrical resistance was measured with Stanford Research Systems lock-in amplifiers and a precision current source at a frequency of a few hertz. The excitation current was usually in the range of 100 nA–10 μA, far below the critical current of the films.

The spectrometer consisted of an Omicron gas discharge lamp operating at the He I resonance line ($h\nu=21.22$ eV) and a modified VSW 150 mm hemispherical electron analyzer fitted with a multichannel detector. The overall resolution was determined to be 9 meV full width at half maximum (FWHM) by fitting the measured Fermi cutoff of a Pt sample at 9 K with a Gaussian (8 meV) and Lorentzian (2 meV) broadened Fermi function corresponding to this temperature. A standard procedure was applied to correct the spectra for the contribution (2.25%) of the He I satellite, but apart from this no other manipulations were performed on the raw data. The determination of the work function of the samples was carried out by taking the difference of the photon energy and the energy difference between the photoelectron secondary cutoff and the Fermi level.[25]

III. RESULTS

Figure 2 shows the behavior of the resistance in time of a C_{60} film at 200 °C that is slowly being doped with potassium, starting from pure C_{60} and ending at K_6C_{60}. The shape of the curve reproduces well between samples with varying thicknesses, and is similar to earlier observations.[26–30] After a quick drop by about one order of magnitude, as the solid solution phase usually called α-C_{60} is formed, the resistance decreases past a kink at about K_1C_{60} to a minimum that is usually identified as K_3C_{60}. This minimum can be extremely sharp, taking only seconds to traverse while the whole doping sequence takes hours, indicating that, at 200 °C substrate temperature, the rate of K diffusion into the film is much higher than the applied doping rate (typically just enough to dope one monolayer of C_{60} to K_3C_{60} per minute), so that good sample homogeneity is achieved. After the minimum, the sample goes through a structural phase transition as it changes from fcc K_3C_{60} to bct K_4C_{60}, and finally ends up at the insulating bcc K_6C_{60} phase, which corresponds to the complete filling of the C_{60} t_{1u} (LUMO) level. The resistance drop near the end is probably due to a partial filling of the C_{60} t_{1g} (LUMO+1) level at the surface. As soon as the dopant flux is reduced to zero, the resistance relaxes to its

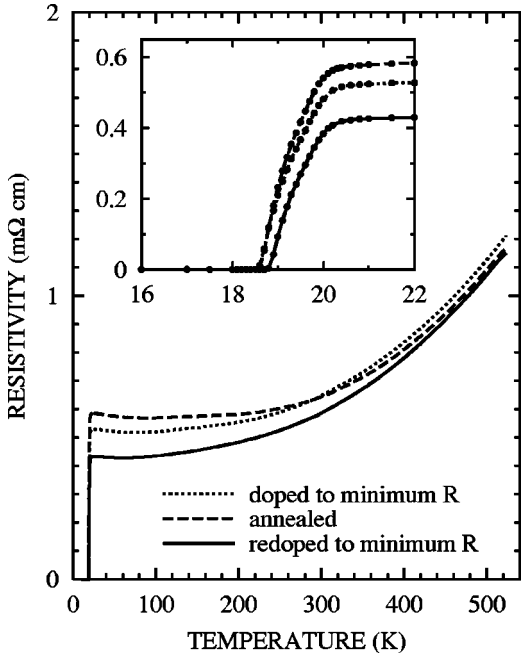

FIG. 3. Resistivity as function of temperature for a 200 nm thick K_3C_{60} film that was K-doped up to the minimum in resistance (dotted curve). After doping, the film was annealed at 250 °C for 54 hours (dashed curve) and doped again to minimum resistance (solid curve). The inset shows an enlargement of the temperature range around T_c.

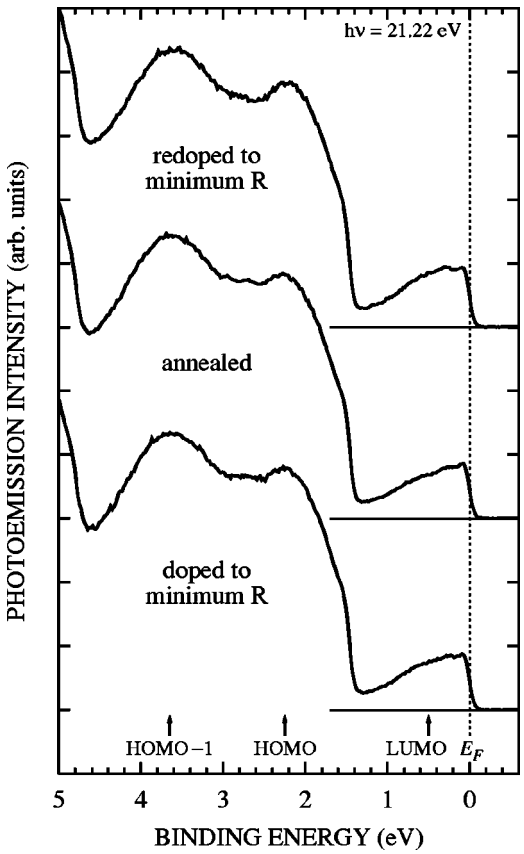

FIG. 4. Room temperature photoemission spectra of the film shown in Fig. 3. Bottom curve: as doped to resistance minimum; middle curve: annealed for 54 hours at 250 °C; and top curve: redoped to new resistance minimum.

final value, which is almost identical to that of the α-C_{60} phase with the lowest K concentration. The vertical equidistant lines in Fig. 2 also show that the time needed to reach the minimum resistance is very close to half the time required to obtain K_6C_{60}, supporting the identification of the resistance minimum with K_3C_{60}.

The temperature dependence of the resistivity of a 200 nm thick K_3C_{60} film, prepared by stopping the doping process precisely at the resistance minimum, is shown in Fig. 3 (dotted curve). The temperature coefficient of the resistivity is positive, i.e., metalliclike, and the film is a superconductor below 19 K. The resistivity just above T_c is ≈ 0.5 mΩ cm, comparable to the lowest values found in K_3C_{60} samples made from C_{60} single crystals.[31] This, and the fact that the superconducting transition is not more than about 1 K wide, can be taken as an indication for the good quality of the sample.

The corresponding photoemission spectrum of this film at room temperature (300 K) is given in Fig. 4 (bottom curve). The line shape of the t_{1u} (LUMO) band clearly shows a sharp and high Fermi cutoff, in good agreement with several of the studies reported in the literature[1–7] and in strong disagreement with some others that hardly show a Fermi cutoff or have a very different t_{1u} line shape.[8–12] We note in addition that, in our film, the height of the Fermi cutoff is the largest so far reported in a photoemission study: we find a ratio of 0.23 for the peak height of the t_{1u}-derived band relative to that of the h_u- (HOMO, or highest occupied molecular orbital) derived band.

To verify that the data correspond to a real equilibrium system, the film was annealed for about 54 hours at 250 °C. We find that after annealing the resistivity just above T_c becomes slightly higher than before [see Fig. 3 (dashed curve)], but that T_c remains the same. Only a very small reduction of the t_{1u} (LUMO) intensity can be observed in the photoemission spectrum as shown in Fig. 4 (middle curve). Surprisingly, by adding now a very small amount of extra potassium onto the film (approximately 0.4% of the initial amount, giving on the average 0.012 extra electrons per C_{60}), we can achieve a new resistivity minimum and improve the conductivity of the film by about 20% near T_c, and even increase T_c by a few tenths of a degree [see Fig. 3 (solid curve)]. This demonstrates the extreme sensitivity of the transport properties of the film to the K concentration in the surface layer, since the amount of added K is negligible as compared to the amount already present in the bulk of the film. In the photoemission spectrum, the extra doping results in an increase of the t_{1u} (LUMO) intensity near the Fermi level: the peak height ratio relative to the h_u (HOMO) band becomes 0.24.

In order to study whether the resistivity minimum corresponds to a maximum in the height of the Fermi cutoff, we have added more potassium to the film, thereby passing the resistivity minimum, and measured the photoemission spectrum. The results are shown in Fig. 5. One can clearly see that the additional doping does not increase the Fermi cutoff height. Instead, a new peak appears at about 0.6 eV binding energy at the expense of the Fermi cutoff intensity. This new peak is a strong signature for the formation of K_4C_{60}, the photoemission spectrum of which is characterized by a

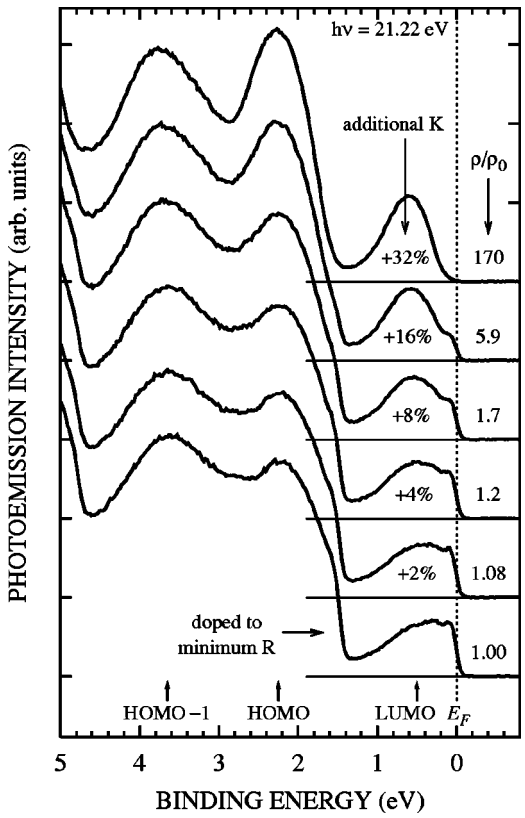

FIG. 5. Room temperature photoemission spectra of a progressively overdoped K_3C_{60} film. The initial film (bottom curve) was obtained by redoping an annealed film (similar to Fig. 4, top curve). The additional amounts of K are approximately, from bottom to top, 0%, 2%, 4%, 8%, 16%, and 32%. The relative resistivity increase ρ/ρ_0 at room temperature (300 K) is indicated, where ρ_0 is the resistivity of the initial film.

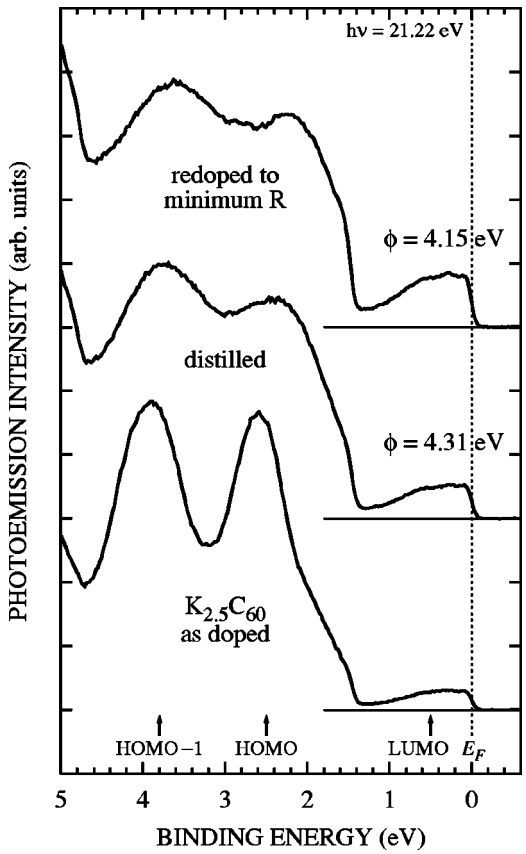

FIG. 6. Room temperature photoemission spectra of a C_{60} film doped to about $K_{2.5}C_{60}$ (bottom). The film was distilled for 60 hours at 250°C (middle) and redoped to minimum resistivity (top). The work function ϕ is indicated for the distilled and redoped films. Initial film thickness was 150 nm.

Gaussian-like feature at 0.6 eV binding energy with a width of about 0.6 eV (Refs. 1–3,5,6). When about $\frac{1}{3}$ extra potassium is added (Fig. 5, top spectrum) the Fermi cutoff completely disappears and the spectrum assumes a typical K_4C_{60} form, while the resistivity increases by a factor of 100 at room temperature and by a factor of 10 at 200°C, consistent with the transition from K_3C_{60} to K_4C_{60} as seen in Fig. 2. It is striking that this process already occurs for the smallest additional doping (2% extra potassium accompanied by 8% increase in resistivity at 300 K). Indeed, it appears that the resistivity minimum corresponds to the highest achievable Fermi cutoff in the photoemission spectrum of K_3C_{60}.

We will now turn to another method that is commonly employed to obtain reproducible K_3C_{60} samples, as described by Poirier *et al.*:[32,33] doping a C_{60} film with potassium to a concentration below K_3C_{60}, followed by a distillation process (or, more accurately, a fractional sublimation process) in order to remove the excess C_{60}. The bottom curve in Fig. 6 shows the photoemission spectrum of a doped C_{60} film with a K concentration of about 2.5 per C_{60} as determined from the time (and therefore doping) dependence of the resistivity of the film as illustrated in Fig. 2 above. We notice that the t_{1u} (LUMO) line shape has a clear and sharp Fermi cutoff, but also that its intensity is quite low: the peak height ratio with respect to the h_u (HOMO) band is only 0.06. The entire spectrum seems to consist of a superposition of C_{60} and K_3C_{60} contributions, suggesting, as has been argued before,[1,5,34,35] that a heavily underdoped K_3C_{60} actually forms a phase-separated system consisting of α-C_{60} and K_3C_{60}. We now distill the film at a temperature of 250 °C. After about 60 hours, no changes in resistance were observed anymore, and we conclude that the sample has reached an equilibrium. This is consistent with other samples where the photoemission spectrum was monitored over time; no significant changes were observed there anymore after several tens of hours. The middle curve in Fig. 6 shows the photoemission spectrum after distillation. The height of the Fermi cutoff has increased considerably, but, surprisingly, is still appreciably smaller than that of the K_3C_{60} films that were made by doping to the resistivity minimum (Fig. 4). The peak height ratio of the Fermi cutoff relative to the h_u (HOMO) band in the distilled K_3C_{60} is a moderate 0.15, and this seems to be a common characteristic of distilled samples: several were prepared, and all of them had peak height ratios in the range of 0.14 to 0.16. These values are consistent with those of the spectra reported in the literature for K_3C_{60} films made in this way.[7]

The temperature dependence of the resistivity of the K_3C_{60} films made by the distillation method is shown in Fig. 7 (dashed line). It reveals quite a large negative temperature coefficient for temperatures below 300 K, and the normal-state resistivity just above T_c is almost a factor of 6 higher than the resistivity-minimum samples of Fig. 3. Also, the

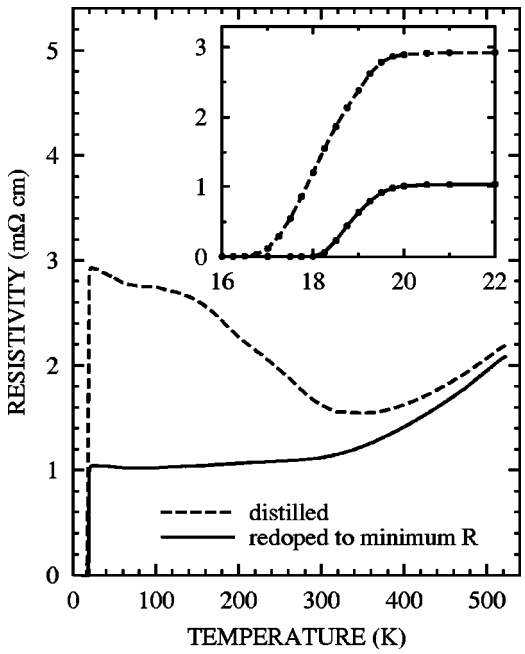

FIG. 7. Resistivity as function of temperature of the distilled and redoped films (dashed and solid, respectively) shown in Fig. 6. The inset shows an enlargement of the temperature range around T_c.

superconducting transition temperature is several degrees lower and the width of the transition is larger, about 2.5 K. This all indicates that the film is more granular, and that the transport properties of the film are strongly determined by tunneling processes across grain boundaries. Nevertheless, the film is still a superconductor, which may be taken as evidence that the bulk of the film is indeed K_3C_{60}.

Now, as we did with the annealed minimum-resistance film before, we add extra potassium to the distilled K_3C_{60} film, and the resistivity drops quickly to reach a minimum after a few minutes. The amount of potassium added is small, about 1.3% of the total amount used to prepare the initial $K_{2.5}C_{60}$ film. The temperature dependence of this redoped film is shown in Fig. 7 (solid line). While the reduction of the resistivity is only 7% at 200 °C, at room temperature (300 K) it is already 30%, and just above T_c the reduction becomes quite dramatic: the conductivity has improved by a factor of 3. The temperature dependence is now metalliclike over the entire temperature range, and the superconducting transition temperature has increased, with a reduced transition width. Redoping has thus improved considerably the transport properties of the distilled film, which now, apart from a somewhat higher absolute value of the resistivity, resembles quite closely those of the minimum-resistivity film described above (Fig. 3). The photoemission spectrum of the redoped film, shown in Fig. 6, reveals that the extra potassium is used to increase the Fermi cutoff intensity. In fact, the peak height ratio relative to the h_u (HOMO) band of this film is now as large as the one of the minimum-resistivity film (Fig. 4), namely 0.24. These results again indicate that the K concentration of the surface layer plays an important role in the properties of the film, since the amount of added potassium is negligible compared to the amount already present in the bulk of the distilled film.

IV. DISCUSSION

The photoemission experiments described above show that there are two distinct, reproducible valence band spectra for K_3C_{60}: one with a LUMO/HOMO peak height ratio of 0.24 using the minimum resistivity method, and one with a ratio of 0.15 using the distillation method. Although one method provides better transport properties than the other, both preparation routes bring us essentially to the superconducting K_3C_{60} compound. At first sight it is surprising that the two photoemission spectra can be that much different, especially since the amount of extra potassium doping that is needed to bring the properties and photoemission spectrum of the distilled sample to those of the minimum resistivity sample is only of the order of 1% of the K concentration in the bulk, not enough to alter the bulk properties significantly. However, one has to realize that photoelectron spectroscopy is a very surface-sensitive technique. Recent ultraviolet photoemission experiments ($h\nu = 21.22$ eV) on noble metal surfaces covered by precisely a single monolayer of (K-doped) C_{60} show that the probing depth is not more than half the diameter of a C_{60} molecule.[36,37] This means that the spectra of the K_3C_{60} films considered here originate essentially only from the outer C_{60} layer. One can now arrive at a very consistent picture in that the differences in the photoemission spectra between the two samples reflect the differences in the surface electronic structure caused by the differences in the potassium concentration in the surface region, which in turn is consistent with the suggestion that most of the extra doping goes into the surface region (or grain boundaries, as discussed below), thereby improving the transport properties of the distilled sample.

In order to understand the electronic structure of the surface, we first have to pay attention to its atomic structure. From all the surface science experiments carried out so far, it seems that pristine C_{60} solids have the close-packed fcc (111) plane as the preferred crystal surface termination. Also upon doping with potassium to K_3C_{60}, the preferred surface termination remains the fcc (111) plane: scanning tunneling microscope (STM) studies show very well ordered and flat triangular lattices,[38–40] and low energy electron diffraction (LEED) measurements show clear 1×1 fcc (111) patterns.[3,7,35,41] Although these observations may seem to be trivial, the consequences are far-reaching and, surprisingly, have gone unnoticed so far. The (111) plane of K_3C_{60} is namely a polar surface, and this constitutes a boundary condition problem of macroscopic dimensions that affects the electronic structure of the surface in a very unique manner. In the subsequent sections we will first discuss the physics of polar surfaces for K_3C_{60} (section A), then the determination of the valence of the C_{60} ions at the surface (section B), and finally the K_3C_{60} surface electronic structure (section C).

A. Polar surfaces

The C_{60} molecules in K_3C_{60} form a close-packed fcc lattice, as shown in Fig. 8(a), with the potassium atoms occupying the octahedral and tetrahedral interstices (1 and 2, respectively, per fullerene). The {111} planes in this crystal structure are special in the sense that they are not charge neutral. Looking along a ⟨111⟩ direction [Fig. 8(b)], we see that these planes form alternating charge planes in the fol-

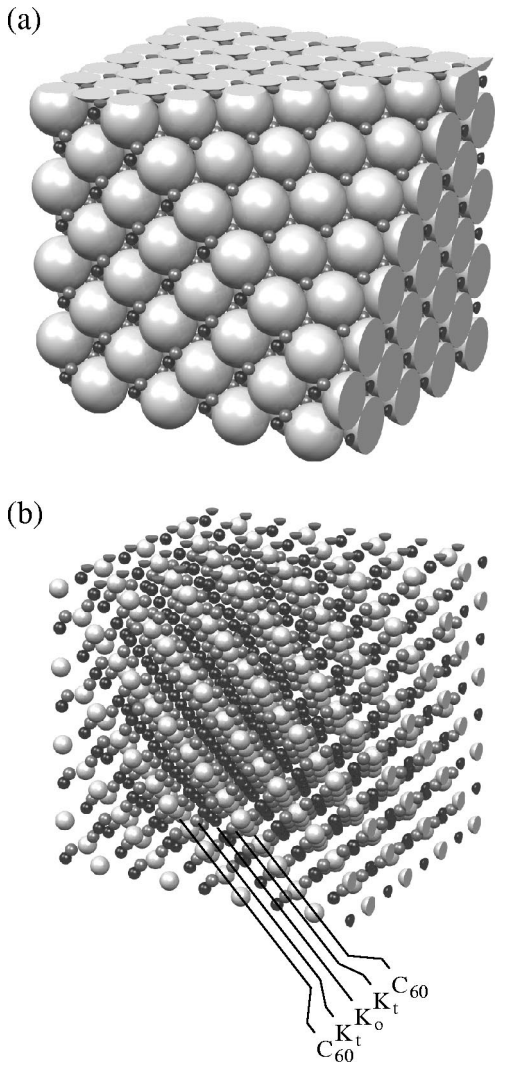

FIG. 8. (a) Structure of a K_3C_{60} crystal. Large spheres represent C_{60} ions, drawn at their van der Waals radius, and small gray and black spheres represent tetrahedral and octahedral potassium ions, respectively. The front, side, and top surfaces of the cube are (100), (010), and (001) planes. The crystal is cut off along the (111) plane, with a (tetrahedral) potassium layer on the outside. (b) The same lattice, with the C_{60} radii reduced. The line of vision is parallel to the (111) plane, showing that the crystal consists of alternating layers of C_{60}, tetrahedral potassium (K_t), octahedral potassium (K_o), tetrahedral potassium (K_t), etc.

lowing sequence: C_{60}^{3-}, K^{1+} (tetrahedral), K^{1+} (octahedral), K^{1+} (tetrahedral), C_{60}^{3-}, etc., all with the same number of ions per unit area. If this K_3C_{60} crystal has the (111) surface as the termination plane, it is subjected to a quite strict and unique boundary condition for its macroscopic charge distribution across the crystal.

This is illustrated schematically in Fig. 9 for a slab consisting of several units of K_3C_{60} planes (of infinite area). The total charge of the slab, of course, has to be zero. If now, for instance, one of two termination planes is a C_{60}^{3-} plane, as drawn in Fig. 9(a), all electric fields between the various planes of the slab point in the same direction, obviously resulting in a net electrostatic potential between the two termination planes. The potential difference increases linearly with the number of K_3C_{60} unit planes, and the potential drop

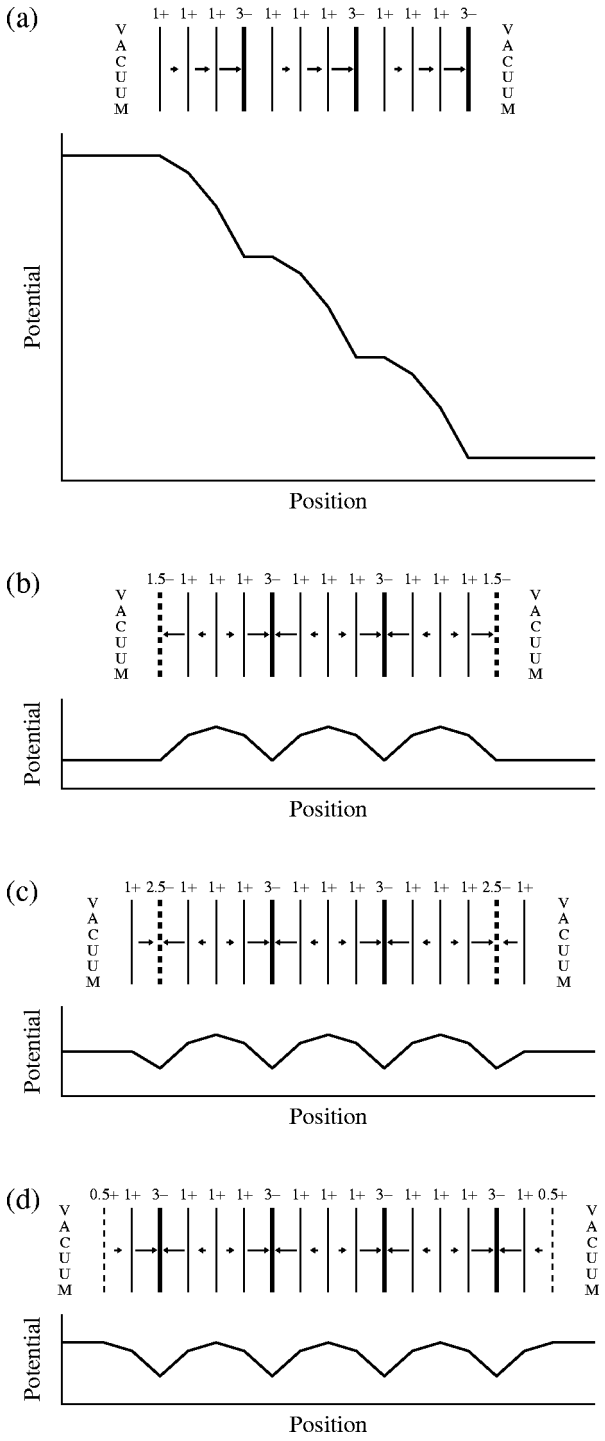

FIG. 9. Schematic view of a finite slab of K_3C_{60} with (111) termination planes. The slab is charge neutral, and within the termination planes it consists of alternating $3-$, $1+$, $1+$, $1+$ charged planes. The termination planes themselves are (a) a C_{60}^{3-} plane on one side; (b) $C_{60}^{1.5-}$ planes; (c) $C_{60}^{2.5-}$ and tetrahedral K^{1+} planes; and (d) C_{60}^{3-}, tetrahedral K^{1+}, and half-populated octahedral K^{1+} planes.

per K_3C_{60} unit is about 25 V. Clearly, no chemical compound can be stable against such potential differences, and certainly not as a macroscopically sized crystal for which the total potential difference between the termination planes can easily end up to be of the order of megavolts. Some form of breakdown must occur to nullify this potential divergence.

We point out that this type of potential divergence is macroscopic in nature, since it is determined solely by the charges of the termination planes and the distance between them. Therefore, surface relaxations, i.e., displacing the atomic positions of the termination planes by (sub)-Ångström distances, cannot solve the divergence if one deals with macroscopic crystals.

To resolve the potential divergence, one has to reduce the charge density of the termination planes to half of the charge of the planes inside the slab. Physically, this can be done in many different ways, and examples can be found from the field of transition metal compounds.[42,43] Neutral-plane facets or ordered defect structures may be formed at the surface (atomic reconstruction),[44–48] differently charged contaminants may get adsorbed at the surface,[48–52] or the valence of the surface atoms becomes different from that of inside the bulk (electronic reconstruction).[53]

In Fig. 9(b) we show a scenario in which the termination planes on both sides are formed by atomically unreconstructed C_{60} surfaces. The valence of the C_{60} ions in those planes is $1.5-$, which is half of $3-$, the value in the bulk. This type of electronic reconstruction gives rise to electric fields inside the slab with alternating signs, so that there is no electrostatic potential difference between the two sides of the slab. In Fig. 9(c) we give another possible scenario for electronic reconstruction: here the termination planes are the tetrahedral K^{1+} planes. The subsurface nearest-neighbor C_{60} planes must then have a valence of $2.5-$, so that the surface K-C_{60} double plane has the required half-charge value of $1.5-$. In Fig. 9(d), by contrast, we show a situation where an atomic reconstruction has taken place: here the termination plane is given by the composite of a full plane of C_{60} with a valence of $3-$, a full plane of tetrahedral K^{1+} and a 50% defect plane of octahedral K^{1+}. Since this surface triple-plane again has an overall valence of $1.5-$, the two sides of the slab are at the same electrostatic potential. In all these scenarios, the outermost C_{60} plane is taken to be not reconstructed atomically, in order to be consistent with the cited scanning tunneling microscopy and low-energy electron diffraction data.[3,7,35,38–41]

B. Surface C_{60} valence

Which of the above mentioned polar surface scenarios is the most likely to occur is difficult to predict *a priori*. It probably depends on the preparation method. It is tempting to associate, for instance, the distilled K_3C_{60} sample with Fig. 9(b) and the minimum-resistivity sample with Fig. 9(c) or 9(d), since the photoemission LUMO intensity and the C_{60} surface valence is appreciably lower in former than in the latter case. It is also tempting to choose Fig. 9(c) rather than 9(d) for the minimum-resistivity sample, since quantitatively, the change in the LUMO/HOMO peak height ratio is from 0.15 to 0.24 in going from the distilled to the minimum-resistivity sample, which fits very well with the change in the surface C_{60} valence from $1.5-$ to $2.5-$ in going from Fig. 9(b) to 9(c).

In order to verify this hypothesis, we have to quantitatively determine the valence of the C_{60} ions of the two K_3C_{60} samples from their photoemission spectra. This can be done with the use of the photoemission spectrum of K_6C_{60} as a calibration for the photoionization cross section of the t_{1u} (LUMO) orbital relative to those of other relevant C_{60} molecular orbitals. The top curve in Fig. 10 displays the valence band spectrum of K_6C_{60}, showing the g_g+h_g (HOMO -1) and the h_u (HOMO) bands together with the t_{1u} (LUMO) band, which is now fully occupied with six electrons per C_{60}. The LUMO is located well below the Fermi level and there is also no intensity at the Fermi level, consistent with the fact that K_6C_{60} is a band insulator. We note that the LUMO/HOMO peak height intensity ratio (0.71) is very high, higher than reported so far in the literature. It turns out that K_6C_{60} is much more difficult to prepare and to measure than K_3C_{60} or K_4C_{60} samples as it is highly reactive. This is probably related to the fact that its work function is very low (measured to be about 2.3 eV), suggesting that its surface is terminated by potassium ions. The ratio between the *integrated* intensity of the LUMO and that of the combined HOMO and HOMO-1 bands is 0.201, as determined from the fits (thin lines) shown in Fig. 10.

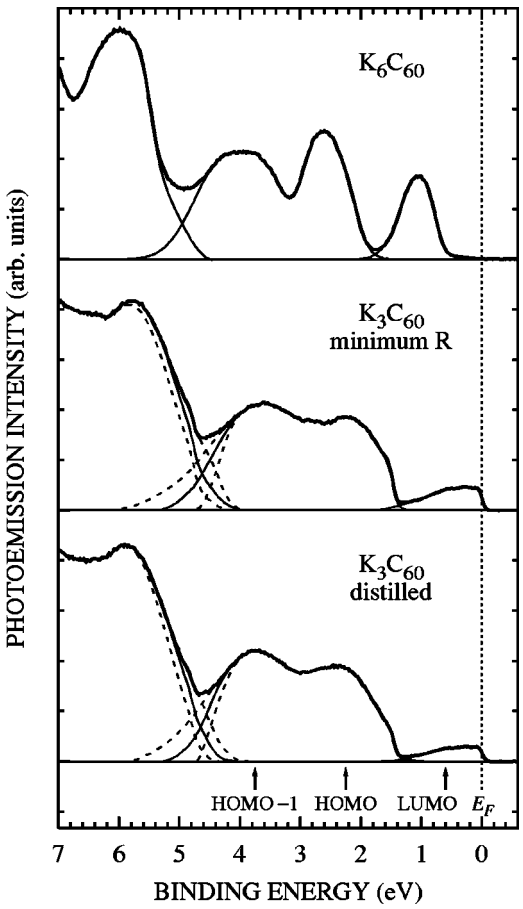

FIG. 10. Determination of the surface valences of the distilled (bottom) and minimum-resistivity (middle) samples. The spectral weight is distributed over three intervals, as indicated by the thin lines: the LUMO (t_{1u}), the combined HOMO (h_u) and HOMO -1 (g_g+h_g), and the rest. The ratios of the integrals over the LUMO and HOMO contributions, normalized to the ratio of a fully doped K_6C_{60} sample (top), yield valencies of $1.5-$ (± 0.1) and $2.5-$ (± 0.2), respectively. The curves corresponding to the error margins are drawn as dashed lines.

For the K_3C_{60} samples, we have determined the integrated intensity ratio of the LUMO with the HOMO and HOMO-1

bands to be 0.050 for the distilled sample and 0.085 for the minimum resistivity sample, using the fits (thin lines) as shown in Fig. 10. Comparing these ratios with the one of K_6C_{60}, which has a C_{60} valence of $6-$, we then find that the C_{60} valence is $1.5-$ (± 0.1) for the distilled sample and $2.5-$ (± 0.2) for the minimum-resistivity sample. The margin of error is mainly determined by the uncertainty in the identification of the line shape of the combined HOMO and HOMO-1 band. The fits drawn with dashed lines in Fig. 10 indicate the range within which this line shape lies, corresponding to the mentioned margin of error. We have also carried out these types of experiments on another photoemission setup, equipped with a different type of electron energy analyzer, and have found the same numbers. These results strongly indicate that the polar surface termination for the distilled sample is indeed given by Fig. 9(b) and the one for the minimum-resistivity sample by Fig. 9(c).

We have measured the work function of the distilled and minimum-resistivity K_3C_{60} samples and found values of 4.31 eV and 4.15 eV, respectively. These values are consistent with the polar surface scenarios discussed above, in the sense that Fig. 9(c) is expected to give a lower work function than Fig. 9(b) due to the presence of an extra layer of tetrahedral potassium ions on top of the outer C_{60} layer. We note that these tetrahedral potassium ions reside in the pockets between the C_{60} ions [see Fig. 8(a)], well below the outer van der Waals surface plane of the C_{60} ions, so they are relatively well protected and also strongly bound. This is much less the case for the octahedral potassium ions in the 50% defect structure of Fig. 9(d), which is perhaps the reason why this structure is not realized. And if this structure would have been realized, then we should at least expect an appreciable decrease of the LUMO intensity after the long annealing process at elevated temperatures of the minimum-resistivity sample, since these loosely bound and exposed octahedral potassium ions would have been removed. The experiment, however, shows a negligible decrease of the LUMO intensity (see the bottom and middle curves in Fig. 4), which is not inconsistent with the finding that there were no outer octahedral potassium ions to begin with.

The fact that the (111) termination plane of K_3C_{60} is found to be electronically reconstructed and not atomically, is perhaps somewhat surprising if one makes a comparison with the case of transition metal oxides where most of the polar surfaces can only be stabilized by facetting or attracting charge contaminants.[44,45,47–52] However, one should not forget that due to its highly degenerate LUMO level and low molecular Coulomb interaction, C_{60} can accomodate any valence in the range of 0 to $6-$, enabling it to form the right boundary conditions all by itself.

C. Surface electronic structure

The finding that the valence of the C_{60} ions at the surface is appreciably different than in the bulk has far-reaching consequences for the electronic structure of the surface. Especially the fact that the valence is not integer but half-integer has a dramatic impact on the properties of the system if the magnitude of various Coulomb interactions is large compared to the one-electron bandwidth. This can be understood as follows.

For a solid with an electronic structure that is characterized by one open shell with an integer valence, one would expect to find an insulating ground state if the one-electron bandwidth (W) is much smaller than the on-site Coulomb energy (U). The one-particle excitation spectrum is then given by a so-called lower Hubbard band in the electron removal part and by an upper Hubbard band in the electron addition part. The two bands are separated by a gap with a magnitude of approximately $U-W$. For solid C_{60}, values of $U \approx 1.6$ eV (Refs. 14, 54, and 55) and $W \approx 0.6$ eV have been measured. Since $U \gg W$, the expectation is that K_3C_{60} should be an insulator just like K_4C_{60} (Ref. 15). The fact that K_3C_{60} is conducting, therefore, is subject of intensive debate, and various models have been proposed, such as including nonstoichiometry[14,17] or including the influence of the occupation-dependent degeneracy of the orbitals on the effective bandwidth[18–23] in order to obtain a conducting ground state.

If the average valence of the solid is not an integer, e.g., due to doping, the system will no longer be an insulator, even if U is much larger than W. The extra hole or electron is then capable to carry charge at a neglible energy cost, and the conductivity is, to a first approximation, proportional to the number of charge carriers. For a half-integer valence one has the highest concentration of charge carriers, and in principle, the highest conductivity.

We would like to point out that the metallicity of the surface is independent of whether the bulk is a metal or an insulator. Also, because the valence is noninteger, the surface is metallic both in a one-particle approximation as well as in a Mott-Hubbard framework. All of these characteristics are the consequence of the electronic reconstruction that precludes the polar surface electrostatic divergence associated with the (111) termination of the fcc lattice.

Finally, we would like to note that the electrostatic considerations for the surface termination on the bulk-vacuum interface are of course also valid for grain boundaries or K_3C_{60}-C_{60} domain interfaces. In fact, the large changes observed in the bulk conductivity, and the temperature dependence thereof, upon the addition of a very small amount of dopant, and its strong correlation with the surface photoemission data, are an indication that grain boundaries play an important role, either due to tunnel barriers between the grains that are strongly modified by changes in the valence at the grain boundaries, or due to a significant part of the electrical conductivity taking place along the metallic grain boundaries themselves. This could be an important aspect, since even single-crystalline C_{60} films or solids become polycrystalline upon doping to K_3C_{60} due to the large change in lattice parameter.

V. CONCLUSIONS

We have carried out combined photoemission and conductivity measurements on K_3C_{60}, and found that the conducting properties are extremely sensitive to the K concentration of the surface layer. The best-conducting samples with the highest superconducting transition temperatures have surfaces with the highest density of states at the Fermi level as measured by photoemission, a technique that probes

essentially only the surface layer due to the very short inelastic mean free path of the outgoing photoelectrons. The K_3C_{60} photoemission spectra are found to be not representative for the bulk: the C_{60} ions at the surface have a stable valence that deviates appreciably from the $3-$ bulk value, namely $2.5-$ or even $1.5-$, depending on the preparation procedure. This is attributed to an electronic reconstruction of the surface to avoid the divergence of the electrostatic potential associated with the polar (111) termination plane of K_3C_{60}. Surfaces or grain boundaries consisting of C_{60} ions with noninteger valence should always be a metal, irrespective of whether the bulk is a metal or a Mott-Hubbard insulator.

ACKNOWLEDGMENTS

It is a pleasure to acknowledge J. Fink, O. Gunnarsson, E. Koch, P. Rudolf, T. T. M. Palstra, and T. Hibma for stimulating discussions. We would like to thank J. C. Kappenburg, M. Mulder, J. F. M. Wieland, R. Hillenga, T. G. Hingst, R. L. Schotanus, and L. Huisman for their skillful technical assistance. This work is supported by the Netherlands Foundation for Fundamental Research on Matter (FOM) with financial support from the Netherlands Organization for Scientific Research (NWO). The research of L.H.T. has been made possible by financial support from the Royal Netherlands Academy of Arts and Sciences.

[1] C. T. Chen, L. H. Tjeng, P. Rudolf, G. Meigs, J. E. Rowe, J. Chen, J. P. McCauley, Jr., A. B. Smith III, A. R. McGhie, W. J. Romanow, and E. W. Plummer, Nature (London) **352**, 603 (1991).

[2] G. K. Wertheim and D. N. E. Buchanan, Phys. Rev. B **47**, 12 912 (1993).

[3] P. J. Benning, F. Stepniak, and J. H. Weaver, Phys. Rev. B **48**, 9086 (1993).

[4] T. Morikawa and T. Takahashi, Solid State Commun. **87**, 1017 (1993).

[5] M. Merkel, M. Knupfer, M. S. Golden, J. Fink, R. Seemann, and R. L. Johnson, Phys. Rev. B **47**, 11 470 (1993).

[6] M. S. Golden, M. Knupfer, J. Fink, J. F. Armbruster, T. R. Cummins, H. A. Romberg, M. Roth, M. Sing, M. Schmidt, and E. Sohmen, J. Phys. Condens. Matter **7**, 8219 (1995).

[7] A. Goldoni, S. L. Friedmann, Z.-X. Shen, and F. Parmigiani, Phys. Rev. B **58**, 11 023 (1998).

[8] T. Takahashi, S. Suzuki, T. Morikawa, H. Katayama-Yoshida, S. Hasegawa, H. Inokuchi, K. Seki, K. Kikuchi, S. Suzuki, K. Ikemoto, and Y. Achiba, Phys. Rev. Lett. **68**, 1232 (1992).

[9] T. Takahashi, T. Morikawa, H. Katayama-Yoshida, S. Hasegawa, and H. Inokuchi, J. Phys. Chem. Solids **53**, 1699 (1992).

[10] T. Takahashi, T. Morikawa, H. Katayama-Yoshida, S. Hasegawa, H. Inokuchi, K. Seki, S. Hino, K. Kikuchi, S. Suzuki, K. Ikemoto, and Y. Achiba, Physica B **186-188**, 1068 (1993).

[11] M. de Seta and F. Evangelisti, Phys. Rev. Lett. **71**, 2477 (1993).

[12] M. de Seta and F. Evangelisti, Phys. Rev. B **51**, 1096 (1995).

[13] S. C. Erwin and W. E. Pickett, Science **254**, 842 (1991).

[14] R. W. Lof, M. A. van Veenendaal, B. Koopmans, H. T. Jonkman, and G. A. Sawatzky, Phys. Rev. Lett. **68**, 3924 (1992).

[15] M. Knupfer and J. Fink, Phys. Rev. Lett. **79**, 2714 (1997).

[16] S. C. Erwin, in *Buckminsterfullerenes*, edited by W. E. Billups and M. A. Ciufolini (VCH, New York, 1992).

[17] J. van den Brink, R. Eder, and G. A. Sawatzky, Europhys. Lett. **37**, 471 (1997).

[18] O. Gunnarsson, E. Koch, and R. M. Martin, Phys. Rev. B **54**, R11 026 (1996).

[19] O. Gunnarsson, E. Koch, and R. M. Martin, Phys. Rev. B **56**, 1146 (1997).

[20] O. Gunnarsson, S. C. Erwin, E. Koch, and R. M. Martin, Phys. Rev. B **57**, 2159 (1998).

[21] E. Koch, O. Gunnarsson, and R. M. Martin, Phys. Rev. Lett. **83**, 620 (1999).

[22] E. Koch, O. Gunnarsson, and R. M. Martin, Phys. Rev. B **60**, 15 714 (1999).

[23] J. E. Han, E. Koch, and O. Gunnarsson, Phys. Rev. Lett. **84**, 1276 (2000).

[24] U. D. Schwarz, W. Allers, G. Gensterblum, J.-J. Pireaux, and R. Wiesendanger, Phys. Rev. B **52**, 5967 (1995).

[25] See, e.g., S. Hüfner, *Photoelectron Spectroscopy* (Springer, Berlin, 1996).

[26] G. P. Kochanski, A. F. Hebard, R. C. Haddon, and A. T. Fiory, Science **255**, 184 (1992).

[27] P. J. Benning, D. M. Poirier, T. R. Ohno, Y. Chen, M. B. Jost, F. Stepniak, G. H. Kroll, J. H. Weaver, J. Fure, and R. E. Smalley, Phys. Rev. B **45**, 6899 (1992).

[28] F. Stepniak, P. J. Benning, D. M. Poirier, and J. H. Weaver, Phys. Rev. B **48**, 1899 (1993).

[29] R. C. Haddon, A. S. Perel, R. C. Morris, S.-H. Chang, A. T. Fiory, A. F. Hebard, T. T. M. Palstra, and G. P. Kochanski, Chem. Phys. Lett. **218**, 100 (1994).

[30] R. W. Lof, H. T. Jonkman, and G. A. Sawatzky, Solid State Commun. **93**, 633 (1995).

[31] J. G. Hou, V. H. Crespi, X.-D. Xiang, W. A. Vareka, G. Briceño, A. Zettl, and M. L. Cohen, Solid State Commun. **86**, 643 (1993).

[32] D. M. Poirier, Appl. Phys. Lett. **64**, 1356 (1994).

[33] D. M. Poirier, D. W. Owens, and J. H. Weaver, Phys. Rev. B **51**, 1830 (1995).

[34] D. M. Poirier and J. H. Weaver, Phys. Rev. B **47**, 10 959 (1993).

[35] P. J. Benning, F. Stepniak, D. M. Poirier, J. L. Martins, J. H. Weaver, L. P. F. Chibante, and R. E. Smalley, Phys. Rev. B **47**, 13 843 (1993).

[36] L. H. Tjeng, R. Hesper, A. C. L. Heessels, A. Heeres, H. T. Jonkman, and G. A. Sawtazky, Solid State Commun. **103**, 31 (1997).

[37] B. W. Hoogenboom, R. Hesper, L. H. Tjeng, and G. A. Sawatzky, Phys. Rev. B **57**, 11 939 (1998).

[38] Y. Z. Li, M. Chander, J. C. Patrin, J. H. Weaver, L. P. F. Chibante, and R. E. Smalley, Science **253**, 429 (1991).

[39] J. H. Weaver, D. M. Poirier, and Y. B. Zhao, in *Electronic Properties of Fullerenes*, edited by H. Kuzmany, J. Fink, M. Mehring, and S. Roth (Springer, Berlin, 1993), p. 146.

[40] P. Jess, U. Hubler, S. Behler, V. Thommen-Geiser, H. P. Lang, and H.-J. Güntherodt, Synth. Met. **77**, 201 (1996). This work refers to Rb_3C_{60} samples, which are in almost all respects identical to K_3C_{60} samples.

[41] A. Goldoni, L. Sangaletti, F. Parmigiani, S. L. Friedmann, Z.-X.

Shen, M. Peloi, G. Comelli, and G. Paolucci, Phys. Rev. B **59**, 16 071 (1999).
[42] P. W. Tasker, J. Phys. C **12**, 4977 (1979).
[43] C. Noguera, *Physics and Chemistry at Oxide Surfaces* (Cambridge University Press, Cambridge, 1996), Sec. 3.3.
[44] V. E. Henrich, Surf. Sci. **57**, 385 (1976).
[45] H. Onishi, C. Egawa, T. Aruga, and Y. Iwasawa, Surf. Sci. **191**, 479 (1987).
[46] C. A. Ventrice, Jr., T. Bertrams, H. Hannemann, A. Brodde, and H. Neddermeyer, Phys. Rev. B **49**, 5773 (1994).
[47] H. Hofmeister, S. Grosse, G. Gerth, and H. Haefke, Phys. Rev. B **49**, 7646 (1994).
[48] D. Cappus, M. Haßel, E. Neuhaus, M. Heber, F. Rohr, and H.-J. Freund, Surf. Sci. **337**, 268 (1995).
[49] H. H. Heikens, C. V. van Bruggen, and C. Haas, Jpn. J. Appl. Phys. **19**, 399 (1980).
[50] N. Floquet and L. C. Dufour, Surf. Sci. **126**, 543 (1983).
[51] F. Rohr, K. Wirth, J. Libuda, D. Cappus, M. Bäumer, and H.-J. Freund, Surf. Sci. **315**, L977 (1994).
[52] M. Hassel and H.-J. Freund, Surf. Sci. **325**, 163 (1995).
[53] A. Fujimori, F. Minami, and N. Tsuda, Surf. Sci. **121**, 199 (1982).
[54] P. A. Brühwiler, A. J. Maxwell, A. Nilsson, N. Mårtensson, and O. Gunnarsson, Phys. Rev. B **48**, 18 296 (1993).
[55] R. Hesper, L. H. Tjeng, and G. A. Sawatzky, Europhys. Lett. **40**, 177 (1997).